Chapter 5

PECVD Amorphous Silicon Carbide (α-SiC) Layers for MEMS Applications

Ciprian Iliescu and Daniel P. Poenar

Additional information is available at the end of the chapter

http://dx.doi.org/10.5772/51224

1. Introduction

Silicon carbide (SiC) became an important material whose popularity has been constantly increasing in the last period due to its excellent mechanical, electrical, optical and chemical properties, which recommend it in difficult and demanding applications.

There are two main fields of applications of SiC. The first one is related to nano electronic [1] or even integrated circuits [2] which are using SiC (in monocrystalline or –sometimes- polycrystalline form) as basic structural material for high frequency [3], high power [4], high voltages [5], and/or high temperature devices [6] or combinations thereof [7]. In most of these applications, SiC act as are placement material for silicon which cannot be used under such extreme conditions.

The second area of applications is related to sensors [8] and actuators, i.e. structures, devices, and/or Microsystems realized (or at least embedding some elements of) micro- and nano electro mechanical systems (MEMS & NEMS). In this area, the usage of SiC (but mainly in polycrystalline and amorphous form) is mainly due to its compatibility and easy integrability with Si and Si-based microfabrication technology. In this direction, a lot of miniaturized devices, such as chemical sensors [9], UV detectors [10], MEMS devices [11-13], and even NEMS [14], are using SiC thin films or substrates (6H-SiC or 4H-SiC).

Polycrystalline-SiC (3C-SiC) thin films can be heteroepitaxially grown on Si substrates [14] due to the deposition temperature well below the Si melting point. [15] However, most of MEMS applications require thin films deposition methods at lower temperatures. This is necessary in order to ensure an overall low thermal budget for the entire fabrication of the SiC-based device(s), an essential prerequisite for postprocessing of MEMS structures on top of Si CMOS circuits, which ensures implementation of 'smart sensors'. Plasma enhanced chemical vapor deposition (PECVD) of SiC in an amorphouos state (α-SiC) can be such a

solution. Early studies have been done on the structural, optical and electronic properties of this material [16, 17]. More specifically, one of the key challenges for PECVD of SiC for MEMS and NEMS applications is achieving alow residual stress together, if possible, with a high deposition rate and good uniformity [16], [18-20].

The main advantages of PECVD α-SiC deposition can be summarized as follows:

- Low temperature deposition, usually between 200-400^{0}C (depending on the specific s of the machine and recipe employed for the deposition, as well as on the details of the device's fabrication process).
- As a direct consequence of the advantage mentioned previously, α-SiC is a highly suitable structural layer for surface micro machining applications using polyimide [21], amorphous silicon [22] or SiO_2 [23] as sacrificial layer materials.
- Stress control in a wide range (e.g. between −1200MPa and 400MPa [24] by tuning of deposition parameters [25], doping [26] or annealing [27].
- The ability of the fabricated device to operate at relatively high temperatures.
- Large mechanical strength of the deposited α-SiC layer.
- Wide bandgap for the deposited α-SiC layer, making it an almost ideal optoelectronic material, transparent for all visible wave lengths above 0.5μm and thus highly suitable for guiding light in the visible and infrared optical spectrum [28].
- A refractive index greater than 2.5 (significantly larger than that of SiO_2 and even that that of Si_3N_4) also make α-SiC an excellent candidate for optical waveguides [29].
- Capability to deposit conformal layers [30].
- The deposited α-SiC has a coefficient of thermal expansion (CTE) relatively similar with that of Si. This means that the risks of both developing very high internal stress within the film and, therefore, of subsequent delamination, are minimized [31] when the devices are operated even at high temperatures.
- The deposited α-SiC is highly suitable for applications requiring a high level of corrosion resistance and moderate operating temperatures (below 300^{0}C) [32].

This chapter will focus on the PECVD deposition of α-SiC layers for MEMS/NEMS applications. The chapter is organized in three major parts:

- A detailed description of the typical PECVD reactor and of the important aspects necessary for a competitive α-SiC deposition process.
- The influence of main parameters on the deposition process and how one could achieve a low stress α-SiC film with anexcellent uniformity and a good deposition rate
- Post-deposition processing of the PECVD α-SiC layerfor various devices and applications.

http://dx.doi.org/10.5772/51224

2. PECVD reactors

The deposition of α-SiC layers in a Plasma Enhanced Chemical Vapor Deposition (PECVD) reactor is facilitated by the plasma generated between two electrodes (radio frequency-RF- or DC discharge) in the presence of reacting gases, the substrate being connected at one of these electrodes. There is a very large diversity of types of PECVD reactors on the market, either for industrial applications or specially designed for dedicated R&D. Usually the R&D equipments are more complex but also may allow much more of flexibility and degrees of freedom in controlling the deposition, thus enabling to obtain different layers with distinct properties using the same reactor.

The key elements in the selection of a PECVD reactor can be summarized as follows:

Deposition chamber. The operating temperature for most of the PECVD reactors is between 200-400°C. In order to achieve a uniform deposition special attention has to be paid to the inlet of the reactive gases, which can be of three types: several inlets around the bottom chuck (electrode), or one inlet through the top electrode, or multiple inlets (shower) from the top electrode. The last solution seems to ensure a better distribution of reactive gases between the working electrodes with positive effect on the film's uniformity. Meanwhile, preheating the gases (using a heated gas distribution system) before their actual introduction into the deposition chamber may also improve the deposition uniformity. Heating the deposition chamber itself (usuallyat 50-100°C) generates gradients of temperature that avoid particle deposition on the substrate during processing. Of course, adding all these elements into a standard system would finally be reflected in a higher cost of the tool.

Loadlock system. Two types of reactors can be distinguished, depending on whether a loading system is present or not: open systems (without lock load, i.e. relatively cheap reactors used only in research labs) and closed systems. The presence of a vacuumed loading system is also a critical element for good PECVD deposition, for a stable and repetitive process. There are two main aspects related to the presence of the load lock: one is related to safety while the other one is related tothe quality of the deposited layer. For the safety aspect, the presence of the loading system avoids the contact of the operator with the by-products resulted during processing, some of which are carcinogenic. As for the process quality, the fact that the chamber is kept permanently under vacuum results in excellent film quality with outstanding reproducibility.

Reconfiguration of the chamber. Cleaning of the chamber is also an important element in achieving good-quality layers. Most of the PECVD reactors also allow a „plasma cleaning" process, which is applied once a certain thickness of the deposited layer is achieved (usually 5-10μm). This cleaning process is designed to remove the products deposited on the chamber's walls or on electrodes, and it is performed mainly using CF_4/O_2 or C_4F_8/O_2 as reactive gasses. The process is followed by a short pre-deposition of the material desired to be deposited in the reactor. Mechanical cleaning must be also performed periodically.

Gas precursors. The PECVD systems frequently used in R&D are equipped with a large number of inlets for the reactive gases. In most of the cases, the equipment is used for multiple depositions such as SiO_2 (doped and undoped), Si_3N_4, α-Si or even TEOS (using a special

Liquid Delivery System –LDS). In our case, for the deposition of α-SiC layers, silane (SiH_4) and methane (CH_4) are the most often used gas precursors, although other precursors, e.g. methyltrichlorosilane (MTCS) [33] or SiH_4/acetylene (C_2H_2) [34], were also studied.

3. Influence of the deposition parameters

3.1. Materials and Methods

This section describes the influence of the main deposition parameters on the film properties, being a practical guide of parameter selection for a desired characteristic of the deposited α-SiC thin film. The experiments were performed on 4 inch diameter, *p* type, 500μm-thick silicon wafers with a (100) crystallographic orientation. The wafers were initially cleaned in piranha (H_2SO_4:H_2O_2 in the ratio of 2:1) at 120°C for 20 minutes and rinsed in DI water. The native silicon oxide layer was then removed by immersing the wafers in a classical BOE solution for 30 seconds. Stress measurement was performed using a KLA Tencor FLX-2320 system while the thickness and thickness uniformity of the thin filmswere measured with a refractometer (Filmetrics F50, USA). The deposition of the tested α-SiC layers was performed using a STS Multiplex Pro-CVD PECVD system described in detail elsewhere [35, 36]. This system enables two RF deposition modes: a low frequency (LF) mode at 380 kHz with a tuning power between 0 to 1 kW, and/or a high frequency (HF) mode at 13.56 MHz with a selected power in the range between 0 to 600 W. The depositions of the α-SiC layers were performed using pure SiH_4(pure) and CH_4 as precursors, with Ar as an overall dilution gas.

3.2. Pressure

The α-SiC deposition's uniformity is strongly dependent on the pressure in the reactor chamber (Fig. 1a).

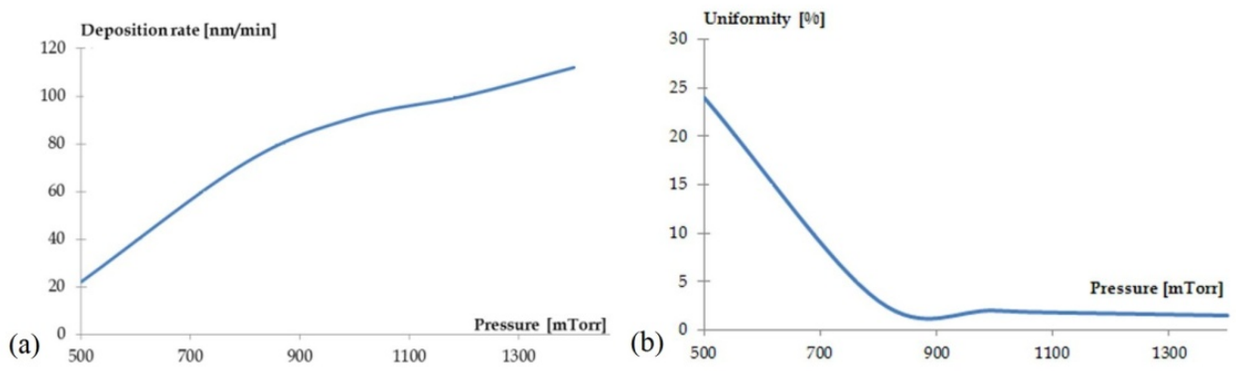

Figure 1. Variation of: (a)uniformity, and (b)deposition rate, with the pressure for α-SiC PECVD deposition in a STS Multiplex Pro-CVD PECVD system.

Below 800mTorr, large non-uniformity values were observed, but the deposition uniformity linearly improved as the pressure was varied between 500 to 800mTorr, finally settling to a

constant valueof the uniformities under 2% for all the pressures in the range 900 to 1400mTorr. The thickness uniformity's map presented a "donut" shape, which means that the gas molecules present a high velocity, increasing the deposition rate at the edge of the wafer.

Another important aspect of the pressure is its influence on the deposition rate (Fig. 1b): low pressures reduce the concentration of reactive species thus resulting in a low deposition rate, which increases quasi-linearly with pressure.

3.3. RF Power

Both the RF power and the power deposition mode are key parameters for tuning the optical and mechanical properties of the deposited PECVD α-SiC layer. A low value of the residual stress is required in MEMS applications where free standing structure is fabricated. Meanwhile, a high deposition rate is desired mainly in industrial applications. Fig. 2 illustrates the variation of the deposition rate and residual stress versus the RF power for the HF mode. The linear dependence of the deposition rate on the HF power noticed for power levels below 300W can be explained by the proportional increase in the dissociation of reactant gases with increasing the power. After a 'threshold' value (300W) the dissociation into reactive species is no longer a crucial factor as probably all reactive species are easily and fully dissociated, hence further increasing the power has little effect on the deposition rate.

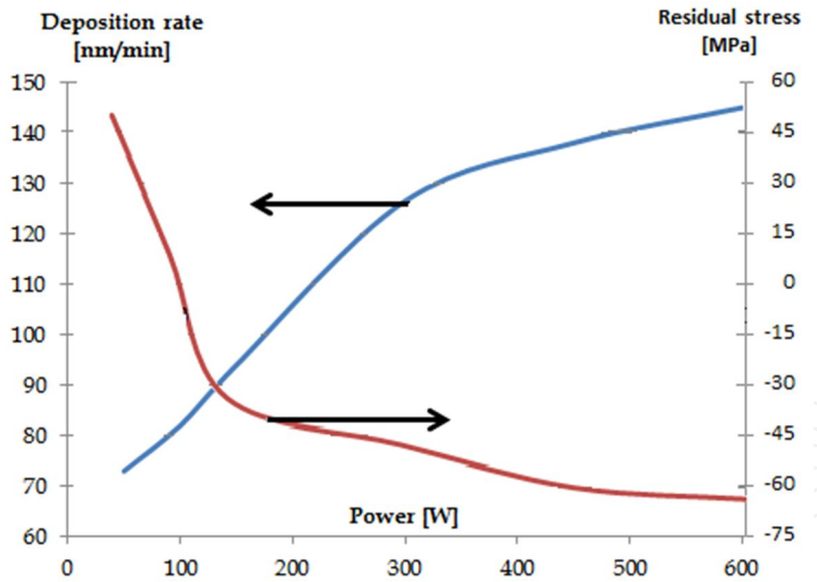

Figure 2. Variation of the deposition rate and residual stress with the HF power in the STS Multiplex Pro-CVD PECVD reactor. The deposition temperature was 300°C, the pressure 1100mTorr, and the gas flow rates of SiH_4, CH_4 and Ar were 45, 300 and 700sccm, respectively.

An interesting characteristic of PECVD α-SiC thin films deposited using the dual mode technique, particularly when compared to other PECVD deposition methods, is the very low value of the internal average stress, which can range between 50MPa and −70MPa. Fig. 2 shows the variation of this residual average with the RF power. Our results indicate that the

average stress variation of a α-SiC film deposited in the HF deposition regime is not due to modifications of the film's chemical composition, but rather due to internal structural re-arrangement because the increasingly higher values of HF power quickly provide enough energy for the adsorbed species to migrate and find the more energetically favorable sites for the film growth to take place.

The refractive index was almost constant in the range between 2.5 and 2.6 while the uniformity of the deposition and uniformity of the refractive index was below 1.5%.

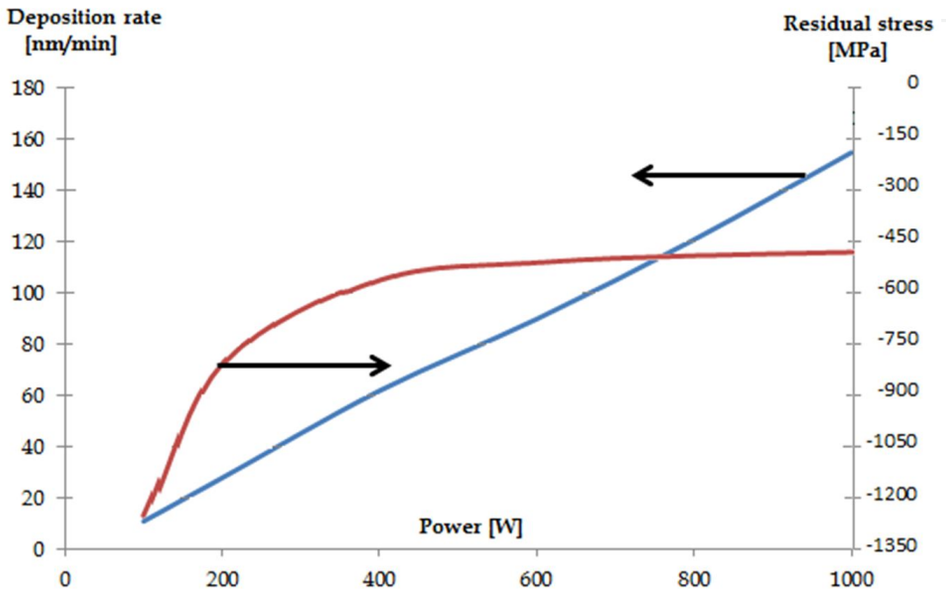

Figure 3. Variation of the deposition rate and residual stress with the LF power in the same PECVD reactor under the same conditions as in Fig. 2.

The variation of the deposition rate and residual stress of PECVDα-SiC films deposited in LF mode are presented in Fig. 3. The differences between HF mode and LF mode are quite evident if one compares the results shown in Fig. 3 with those shown in Fig. 2. The deposition rate depends linearly with the LF power. However, for low values of LF power, the stress is highly compressive (even below −1200MPa) but quickly reduces to about −500MPa and remains almost constant at this value for any LF power above 300W. This variation can be explained by the densification of the layer determined by the increasingly more energetic ion bombardment with increasing the LF power, which characterizes the LF deposition mode. At high frequencies, only the electrons are able to follow the RF field while the ions cannot follow the instantaneous variations of the electric field due to their heavier mass. The cross over frequency at which the ions start following the electric field is between 1 and 5MHz depending upon the mass of the ions. Consequently, below 1MHz, the ion bombardment is significantly higher, which not only enhances chemical reactions but also densifies the film. However, the refractive index of α-SiC film decreases with the increasing the LF power (from 2.9 to 2.5). It can be concluded that, for a low value of the residual stress in the α-SiC layers, the HF deposition mode is more suitable. Meanwhile, the HF mode assures a

better dissociation of the gasses that is reflected in a higher deposition rate.The deposition in LF mode is more suitable when PECVD α-SiC is used as masking layer or in applications for harsh environments (due to the densification of the layer).

3.4. Temperature

A very interesting characteristic of the PECVD α-SiC deposition in the LF mode and which can be useful in many applications is that the deposition rate as well as the residual stress do not present relevant variations as a function of temperature [37]. In contrast, in the HF mode, temperature has an important effect on the stress value, although the deposition rate is not much affected by temperature in HF mode as well [37]. As is depicted in Figure 4, the internal average stress is compressive (around −110MPa) when the α-SiC layers are deposited at 200°C, but it becomes more and more tensile with increasing the deposition temperature,the stress (for temperature between 350 and 400°C). Most remarkable is the fact the stress is very low (around zero) when the deposition temperature is situated between 300 and 350°C.

The refractive index value remained almost constant at 2.6 for all the films deposited in the HF mode which proves that the stress variation is resulted from the film's structural re-arrangement, not from modifications of its chemical composition [37].

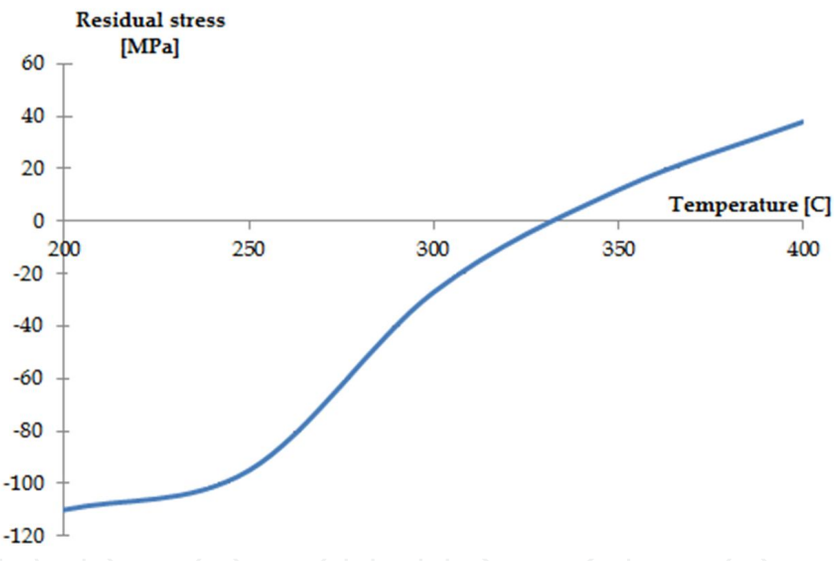

Figure 4. Variation of the average residual stress of PECVD α-SiC films with the deposition temperature. The films were deposited in the HF mode at a power of 150W, at a pressure of 1100mTorr, and with gas flow rates of SiH_4, CH_4 and Ar of 45, 300 and 700sccm, respectively.

3.5. SiH_4/CH_4 ratio

The influence of the SiH_4/CH_4 gas flow ratio, illustrated in Fig. 5, shows a linear dependence of the (compressive) residual stress on the SiH_4/CH_4 ratio for depositions in the HF mode. As expected, increasing the SiH_4 content from 1:10 to 2:10 in the gas flow makes the deposited α-SiC film more „Si-rich" and at the same time decreases the magnitude of

the compressive stress from about −70MPa to −20MPa, while at the same time the refractive index increases from 2.6 to 2.8.

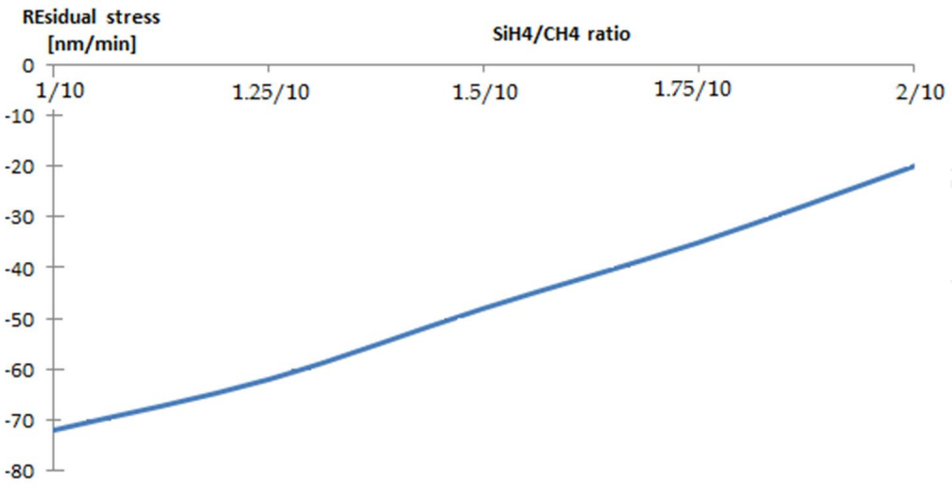

Figure 5. Variation of the average residual stress with the SiH_4/CH_4ratio for PECVD α-SiC films deposited at 300°C. The SiH_4 flow rate was kept constant at 45sccm, while all the other deposition conditions were the same as those indicated in Fig. 4.

To conclude, an optimized process recipe for the deposition of a low stress α-SiC film using a STSP PECVD reactor has the following parameters:

Process parameters/ Characteristic of the deposition process	Value
Pressure	1400mTorr
Power (HF mode)	600W
SiH_4, CH_4 and Ar gas flows	70, 500, and 700sccm
Deposition temperature	400°C
Refractive index	2.62
Residual Stress	± 5MPa
Deposition rate	180nm/min
Uniformity (refractive index & thickness)	<1%

Table 1.

4. MEMS application of PECVD α-SiC layers

4.1. Patterning of SiC layers

Micro patterning of thin α-SiC film layer deposited in PECVD reactor is similar to the patterning of crystalline or polycrystalline SiC layers. The patterning can be done in Reactive Ion Etch-

ing (RIE) or Inductive Coupled Plasma (ICP) deep RIE (DRIE) equipments by fluorine chemistry, i.e. using a fluorine-containing gas (CF_4,SF_6 or even CHF_3) and O_2 and using photoresist as masking layer. It must be mentioned that the selectivity of the etching process to Si (used as substrate), SiO_2, or even to photoresist is not outstanding (ranging from 1.2 up to 0.5) [16]. Metal masking layers have thus been initially been choosen [38, 39]. However, metal masks cause a major problem, namely the micromasking effect: as dry etching progresses, metallic particles are extracted from the mask and re-deposited onto the film/substrate where they can continue to have a protective role, resulting in a very uneven and rough final surface. For instance, aNF_3/O_2 chemistry was tested for etching a SiC layer [40] using to photoresist is mask, achieving etching rates of 0.135μm/min. Similarly, HBr/Cl_2 etching chemistries using SiO_2 etch masks have been developed [41]. This latter chemistry allowed a high selectivity (20:1) of etching SiC with respect to SiO_2, but the price to pay was a very low etching rate (0.02μm/min). In a more recent work, Senesky and Pisano reported the usage of AlN as masking layer for SiC structures in an ICP DRIE reactor using SF_6/O_2 chemistry [42]. The etching process yielded a SiC etch rate of 0.4μm/min, having a high selectivity (SiC/AlN) of 16:1. Moreover, the anisotropy of the process was very good, as features with a sidewall angle of 10° were reported. In another work,Cl_2 chemistry was used in an ICP DRIE reactor (by Pandraud et al.) for uniform patterning of a PECVD α-SiC layer for wave guide applications [43].

4.2. PECVD α-SiC as masking layer

The intrinsic chemical inertness of SiC makes PECVD α-SiC an interesting candidate as masking layer for harsh wet and dry etching.

4.2.1. Masking layer for orientation dependent etching of Si in alkaline solutions

A low etching rate of 78nm/h of low stress PECVDα-SiC in a 30%KOH solution was reported [19, 24, 37], while etching rates lower than 2nm/h in both 33%KOH at 85°C as well as in 25% TMAH are reported by Sarro in [16]. As expected, the etching rate depends on both the composition of the deposited α-SiC layer and its density. However, in general, the reported results are in the same range with the etch rate values of PECVD Si_3N_4 (13 nm/h) in KOH 20% at 85°C [36] but much better than the etch rate of thermal SiO_2 (462 nm/h)in the same etchant [44]. As the reported etch rates of PECVD α-SiC have such relatively low values, we can conclude that PECVD α-SiC can be successfully used as a mask in silicon bulk micromachining processes. Furthermore, we have practically tested this hypothesis and demonstrated the feasibility of using PECVD α-SiC as masking layer, as is detailed in the next section.

4.2.2. Masking layer for etching in HF based solutions

Deep wet etching of glass is an important technology for microfluidic applications [45]. The main etchant for glass materials is highly concentrated HF [46] (sometimes with a small amount of HCl [47] or H_3PO_4 added [48]). PECVD α-SiC is almost an inert material in these solutions, exhibiting etching rates lower than 10Å/h [37]. Such an extremely low etching rate in highly concentrated HF solutions combined with the reduced value of the stress are the main request of a good masking layer for deep wet etching of glasses [46, 49-51]. In our tests,

a compound masking multilayer 'sandwich' made to low stress α-Si/low stress α-SiC/photoresist seemed to be the best solution in terms of depth of the etch achieved without any damage of the mask (through- etching of 1 mm thick Pyrex glass wafers, equivalent of a 2.5 hour exposure to 49% HF). The experimental results of processing Pyrex glass wafers (Corning 7740) in such a manner are presented in Fig. 6. It can be noticed that the mask is fully intact after the etching process while the shape of the etched hole describes a perfect isotropic process. The α-Si was used in this case as an adhesion layer. If only PECVD α-SiC is used as masking layer, a hugely isotropical etching process can still be observed [50].

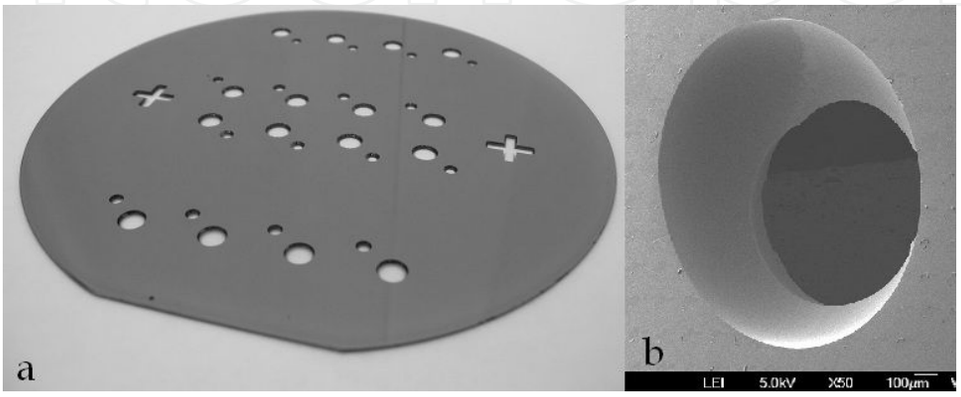

Figure 6. (a) Optical image of a glass wafer coated with PECVD α-Si/PECVD α-SiC/Photoresist after etching through in HF 49%, and (b) a SEM picture of one of the resulted etch-through holes in the glass wafer.

4.2.3. Masking layer for dry release structure in XeF_2

Dry release in XeF_2 is an emerging technology in surface and bulk micromachining of MEMS free-standing structures. The PECVD α-SiC films present a low etching rate in XeF_2 gas (around 7 Å/min) which makes the α-SiC very suitable as a structural layer for any dry-release processes using α-Si or polysilicon as a sacrificial layer. Fig. 7 presents SEM images with PECVD α-SiC cantilevers fabricated using dry released in XeF_2 [24].

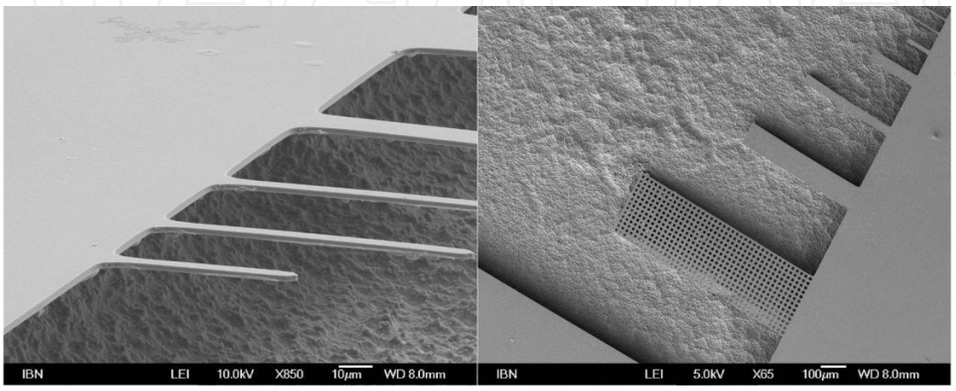

Figure 7. PECVD α-SiC cantilevers fabricated using dry-released process in XeF_2.

http://dx.doi.org/10.5772/51224

4.2.4. Protective layer for harsh environment

PECVD α-SiC films are also very suitable for structures intended to operate in harsh environments, due to α-SiC 's large hardness (2.48kg/m^2) [52], high fracture strength, high modulus [53], excellent wear resistance [54] and chemical inertness in acid or based solutions, low oxidation rate and strong covalent Si-C bonds [52]. Early work proved the potential of PECVD α-SiC as a potential material for encapsulation of micromachined transducers due to its good resistance in a large range of media such as piranha solution, HF and KOH [55].

The good mechanical strength and anti-stiction surface properties of PECVD α-SiC [56] as well as its inertness in corrosive environment recommends this material for diverse applications. An illustrating example is that of a 1μm-thick PECVD α-SiC combined together with Teflon like fluoro-polymer coatings to reduce the demolding energy by a factor of about 10, compared to a bare silicon mold [57]. In another similar application PECVD α-SiC was used for its hardness and for its good step-coverage (improving the wall roughness generated during the deep RIE process) while the Teflon layer acted as an anti-stiction layer [58]. Decreasing the demolding energy, in this application, is equivalent with the increasing of the life-time of the Si mold (used usually for rapid prototyping on hot embossing tools).

In another application [30], a 1μm-thick PECVD α-SiC layer was used as an anti-erosion coating layer of a piezoresistive pressure sensor. In order to reduce the residual stress in the α-SiC protection layer (initially evaluated at −450MPa), annealing was performed at 450°C for 1h. The resulting stress value was of only +60MPa. The α-SiC protective layer also showed a good coverage of the Al metallization layer. The erosion testing was performed in 45%KOH solution at 80°C. The final PECVD α-SiC-coated pressure sensor showed a small decrease in sensitivity, but exhibited a high erosion resistance and less temperature dependence. A similar application was also reported [59], in which low stress PECVD α-SiC layer was used for a capacitive pressure sensor fabricated using surface micromachining. Aluminum was used as material for electrodes while polyimide was selected as a sacrificial layer.

4.3. Fabrication of free standing structuresof PECVD α-SiC using to surface micromachining

The opportunity of using thick α-Si (amorphous silicon) layers [22] (up to 20μm thick, from our own experience) in surface micromachining gives rise to new processing opportunities, especially for microfluidic applications. The α-Si sacrificial layer can be easily removed by wet etching in an alkaline solution (TMAH or KOH) or by dry release in XeF_2. The PECVD α-SiC presents a high chemical inertness to all the etchants of the above mentioned processes, and, therefore, is a very attractive candidate as a structural layer for surface micromachining processes in which amorphous silicon is used as a sacrificial layer. An example of such a process used a 3μm-thick free standing structure fabricated from PECVD α-SiC on a glass substrate using 9 μm-thick PECVD α-Si as sacrificial layer [22]. The structure was released using wet etching in 30% KOH at 80°C. The structure (presented in Fig. 8) shows also that the PECVD deposition process ensured a very good step coverage, the thickness of the vertical wall being identical with that of the layer on the horizontal surfaces [22]. In another example of using PECVD α-SiC as structural material for surface micromachining, 1μm-thick self-sustaining microbridges and microtunnels were fabricated from PECVD α-SiC

films (deposited at 320°C using CH_4 and SiH_4 as reactive gases), using a SiO_xN_yfilm as a sacrificial layer [60]. In a similar manner, self-sustained grids have also been fabricated [61].

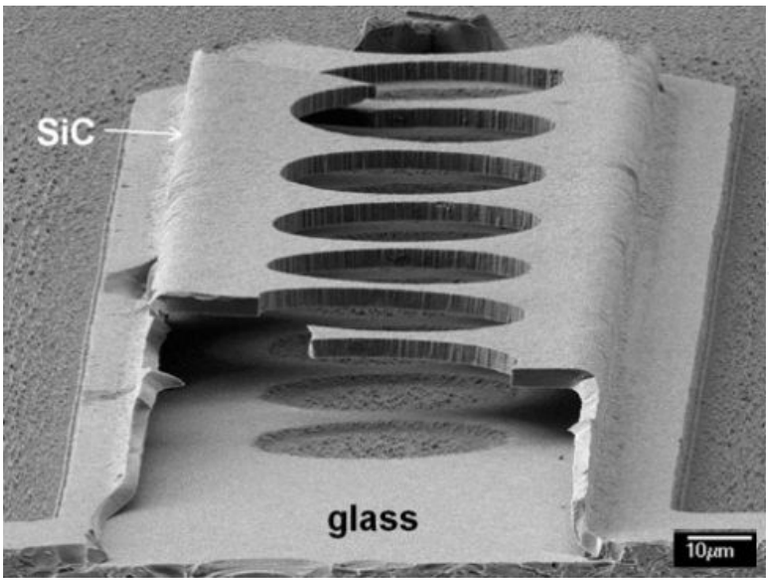

Figure 8. SEM image of asuspended structure fabricated by surface micromachining using thick low-stress α-Si as sacrificial layer and PECVD α-SiC as a structural layer [22].

PECVD α-SiC was used in shunt capacitor RF MEMS microbridge-based switches [23]. In this application 300 nm and 500 nm thick PECVD α-SiC films were used as structural layers, while 2μm-thick PECVD SiO_2 was used as a sacrificial layer. The structures were released in BOE, followed by CO_2 supercritical drying in order to eliminate anysticton possibility. Polyimide was the choice for the sacrificial layer in an application which also used PECVD α-SiC as structural layer [21]. The main advantage of using polyimide is the opportunity of using a dry release process (in O_2 plasma), thus more easily overcoming stiction problems often encountered in wet sacrificial etching technology than by using XeF_2 or CO_2 supercritical drying, solutions which require much more complex and expensive achiness.

4.4. Biological applications of PECVD α-SiC

MEMS materials are suitable for applications in cell culture and tissue engineering [62]. In this direction, a special attention is given to the layers achieved by PECVD deposition especially α-Si_3N_4 [63], [64-66] and α-SiC [37]. The main motivation in using these materials and PECVD as deposition method are related to:

1. Both α-Si_3N_4 and α-SiC can be used for the fabrication of 2-3μm thick membranes using classical micromachining processes.
2. PECVD deposition allows a good control of the residual stress in the layer, a critical aspect in achieving free standing structures.
3. Both α-Si_3N_4 and α-SiC are optically transparent, so the classical inverted microscopes use in biology can be easily used to monitor bio-samples in structures realized with these materials, for example, in assays emplying red/green fluorescence.

http://dx.doi.org/10.5772/51224

4. Using microfabrication, these membranes are attached to a supporting Si ring which makes the structure easy to be handle (comparing with polymeric membranes where no such rim support is present) [66].

5. Porous PECVD α-SiC and α-Si_3N_4 membranes can be fabricated with a good control of the pore size and with a uniform distribution of the pores can be achieved.

6. The commercially available and presently used polymeric membranes are hydrophobic materials, and metabolites (albumin, urea) are absorbed in this membrane with effect on cell viability.

7. The thickness of polymeric porous membrane is usually ranging from tens to hundreds of microns. Consequently, the mass transfer of (bio) chemical substances across/through the membrane is strongly affected by the thickness of the membrane and its nature (hydrophilic/hydrophobic).

8. The presence of functional groups, such as amine (-NH_2), and methyl (-CH_3), on the surface of α-Si_3N_4 and α-SiC membranes can significantly enhance the cell adhesion on these materials.

9. The α-SiC and α-Si_3N_4 membranes can be easily cleaned: complete removal of all organic contaminants can be achieved in piranha solution, followed by subsequent rinsing, drying and if necessary even sterilization can also be performed, in order to ensure complete reusability.

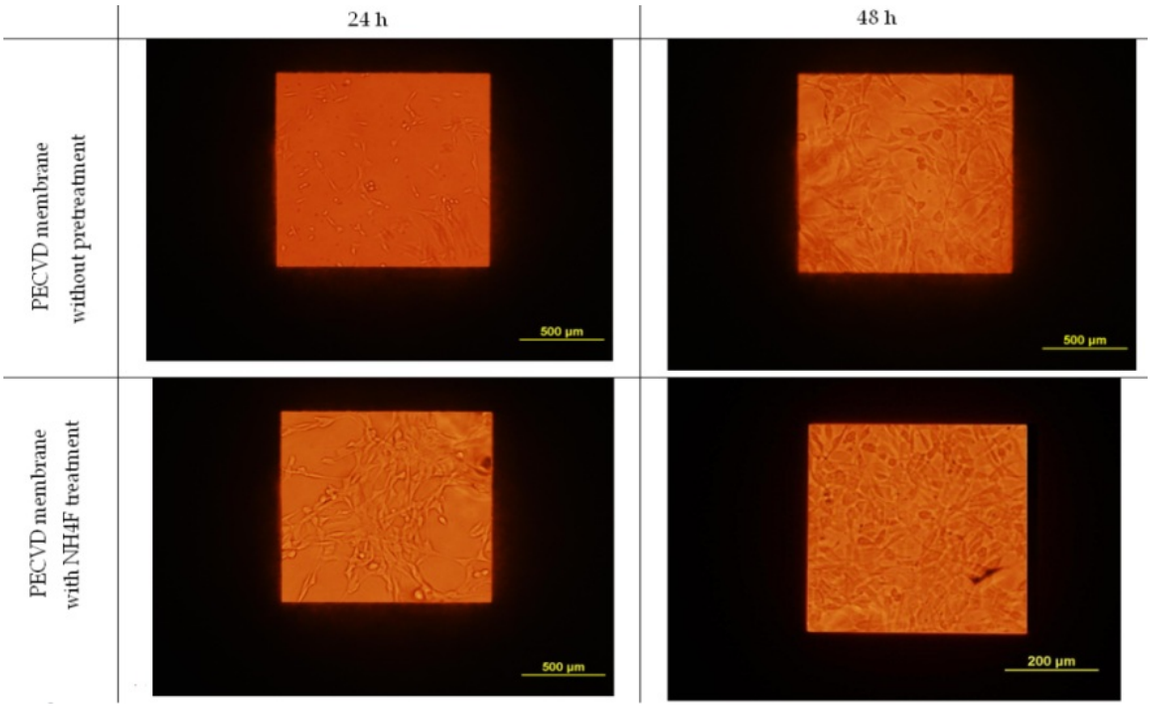

Figure 9. Optical images with the adhesion of fibroblast NIH3T3 cells on PECVD α-SiC membrane treated in NH_4F after 24h and 48h cell culture.

As an illustrative example, chips with 2.5μm-thick PECVD α-SiC membranes were fabricated by bulk micromachining in order to test the biocompatibility of the α-SiC [37]. Fibroblast NIH3T3 cells were used in this study as the model cell line. It was observed that the presence of CH_3 groups on the surface of the membranes improved the cell adhesion. Moreover, dipping for 1 minute in 40% NH_4F, which was performed mainly to reduce the density of native silicon oxide groups on the α-SiC surface, also improved the adhesion of the cells on the membranes' surfaces. Fig. 9 shows cell culture images taken 24 hours and 48 hours after starting the culturing.

5. Concluding remarks

We can conclude that PECVD α-SiC is a very attractive and promising material. Its PECVD deposition enable low temperature processing and thus ensures compatibility with CMOS processing, which is essential when (bio) MEMS/NEMS structures need to be combined together with signal processing and data conditioning circuits, a *sine qua non* condition of realizing "smart sensors". Additionally, PECVD deposition enables the user to modify various deposition parameters (temperature, pressure, precursors gas flow ratios) which can allow the user to optimize –at least in principle- the desired film properties: chemical composition internal average stress and refractive index. However, in practice such multi-dimensional optimization may prove difficult to achieve, and the presence of some extra degrees of freedom is welcome. An example to the point is -in our case- the presence of dual LF and HF modes for the STS Multiplex Pro-CVD PECVD reactor, which provided valuable flexibility in usage and in varying independently various characteristics of the film (e.g. minimizing the stress) without compromising the others (e.g. the refractive index). In some cases, when such a machine is not available, some more maneuvering room is given by adding an anneal process, which always reduces (sometimes significantly) the film's stress.

Application-wise, the long list of extremely desirable properties exhibited by α-SiC (large hardness, high fracture strength, high modulus, excellent wear resistance, superb chemical inertness and excellent stability even at high temperatures and/or under corrosive conditions) ensure it can be used in a very large area of applications, particularly in harsh environments, where Si devices cannot be used. Moreover, the same properties recommend PECVD α-SiC as the material of choice for a large range of MEMS postprocessing fabrication techniques. Thus, it can be used as mold material (or mold-coating protective layer), masking material or active structural material in surface micromachining.

Finally, we should also highlight that α-SiC can has also been employed in bio-related applications. Our own tests have shown that PECVD α-SiC membranes fabricated by bulk micromachining can be used successfully in cell cultures. Here the intrinsic properties of α-SiC ensure very good chemical stability, possibility to easily functionalize the surface for, e.g., increased cell adhesion, and improved mechanical resistance and easy handling.

Author details

Ciprian Iliescu[1*] and Daniel P. Poenar[2]

*Address all correspondence to: ciliescu@ibn.a-star.edu.sg

1 Institute of Bioengineering and Nanotechnology, Singapore

2 Microelectronics Centre, School of Electrical & Electronics Engineering, Nanyang Technological University, Singapore

References

[1] Zhou, W. M., Fang, F., Hou, Z. Y., Yan, L. J., & Zhang, Y. F. (2006). *IEEE Electron Dev. Lett.*, 27(6), 463-465.

[2] Patil, C., Xiao-An, F., Anupongongarch, C., Mehregany, M., & Garverick, S. (2007). *Proc. IEEE Compound Semicond. Int. Circuit Symp.*, 1-4.

[3] Sarazin, N., Morvan, E., di Forte Poisson, M. A., Oualli, M., Gaquiere, C., Jardel, O., Drisse, O., Tordjman, M., Magis, M., & Delage, S. L. (2010). *IEEE Electron Dev. Lett.*, 31(1), 11-13.

[4] Peftitsis, D., Tolstoy, G., Antonopoulos, A., Rabkowski, J., Jang-Kwon, L., Bakowski, M., & Nee, H. (2012). *IEEE Transactions on Power Electr.*, 27(1), 28-36.

[5] Woongje, S., Van Brunt, E., Baliga, B. J., & Huang, A. Q. (2011). *IEEE Electron Dev.Lett.*, 32(7), 880-882.

[6] Nikiforov, V., Tomás García, A. L., Petrushina, I. M., Christensen, E., & Bjerrum, N. J. (2011). *Int. J. Hydrogen Energy*, 36(10), 5797-5805.

[7] Singh, N. B., Wagner, B., Berghmans, A., Knuteson, D. J., Mc Laughlin, S., Kahler, D., Thomson, D., & King, M. (2010). *Crystal Growth & Design*, 10(8), 3508-3514.

[8] Myers, D. R., Cheng, K. B., Jamshidi, B., Azevedo, R. G., Senesky, D. G., Chen, L., Mehregany, M., Wijesundara, M. B. J., & Pisano, A. P. (2009). *J. Micro-Nanolithogr. MEMS MOEMS*, 8(2).

[9] Soo, M. T., Cheong, K. Y., & Noor, A. F. M. (2010). *Sens. Actuator B-Chem.*, 151(1), 39-55.

[10] Borchi, E., Macii, R., Bruzzi, M., & Scaringella, M. (2011). *Nuclear Instruments and Methods in Physics Research Section A: Accelerators, Spectrometers, Detectors and Associated Equipment*, 658(1), 121-124.

[11] Azevedo, G. R., Jones, G. D., Jog, V. A., Jamshidi, B., Myers, R. D., Chen, L., X.-a., Fu, Mehregany, M., Wijesundara, B. J. M., & Pisano, P. A. (2008). *Sens. Actuator A-Phys.*, 145-146(0), 2-8.

[12] Jiang, L., Cheung, R., Hedley, J., Hassan, M., Harris, A. J., Burdess, J. S., Mehregany, M., & Zorman, C. A. (2006). Sens. Actuator A-Phys.(2), 1128(2), 376-386.

[13] Hyun, J. S., Park, J. H., Moon, J. S., Kim, S. H., Choi, Y. J., Lee, N. E., & Boo, J. H. (2005). *Progress in Solid State Chemistry*, 33(2-4), 309-315.

[14] Zorman, A., & Mehregany, M. (2002). *Proc. of IEEE Sensors*, 2, 1109-1114.

[15] Liu, F., Carraro, C., Pisano, A. P., & Maboudian, R. (2010). *J. Micromech. Microeng.*, 20(3).

[16] Sarro, P. M., Deboer, C. R., Korkmaz, E., & Laros, J. M. W. (1998). *Sens. Actuator A-Phys.*, 67(1-3), 175-180.

[17] El Khakani, M. A., Chaker, M., Jean, A., Boily, S., Kieffer, J. C., O'Hern, M. E., Ravet, M. F., & Rousseaux, F. (1994). *J. Mat. Research*, 9(1), 96-103.

[18] Roper, S., Howe, R. T., & Maboudian, R. (2006). *J. Micromech. Microeng.*, 16(12), 2736-2739.

[19] Iliescu, M., Avram, B., Chen, A., Popescu, V., Dumitrescu, D. P., Poenar, A., Sterian, D., Vrtacnik, S., Amon, P., & Sterian, . (2011). *J. Optoel. Adv. Mat.*, 13(4), 387-394.

[20] Sarro, P. M. (2000). *Sens. Actuator A-Phys.*, 82(1-3), 210-218.

[21] Bagolini, L., Pakula, T. L. M., Scholtes, H. T. M., Pham, P. J., French, P. M., & Sarro, . (2002). *J. Micromech. Microeng.*, 12(4), 385-389.

[22] Iliescu, B., & Chen, T. (2008). *J. Micromech. Microeng.*, 18(1), 15024.

[23] Parro, R. J., Scardelletti, M. C., Varaljay, N. C., Zimmerman, S., & Zorman, C. A. (2008). *Solid-State Electronics*, 52(10), 1647-1651.

[24] Iliescu, C., Chen, B. T., Wei, J. S., & Pang, A. J. (2008). *Thin Solid Films*, 516(16), 5189-5193.

[25] Avram, M., Avram, A., Bragaru, A., Chen, B., Poenar, D. P., & Iliescu, C. (2010). *Proc. of the 33rd IEEE Int. Semicond. Conf.*, 239-242.

[26] Pham, H. T. M., De Boer, C. R., Kwakernaak, K., Sloof, W. G., & Sarro, P. M. (2001). *Proc. of SPIE*, 272-279.

[27] Oliveira, R., & Carreno, M. N. P. (2006). *J. Non-Crystalline Solids*, 352(9-20), 1392-1397.

[28] Pandraud, G., French, P. J., & Sarro, P. M. (2008). *Sens. Actuator A-Phys.*, 142(1), 61-66.

[29] Pandraud, G., French, P. J., & Sarro, P. M. (2005). *Microw. Opt. Technol. Lett.*, 47(3), 219-220.

[30] Zhang, H., Guo, H., Wang, Y., Zhang, G., & Li, Z. (2007). *J. Micromech. Microeng.*, 17(3), 426-431.

[31] Slack, G. A., & Bartram, S. F. (1975). *J. Appl. Phys.*, 46(1), 89-98.

[32] Azevedo, R. G., Jingchun, Z., Jones, D. G., Myers, D. R., Jog, A. V., Jamshidi, B., Wijesundara, M. B. J., Maboudian, R., & Pisano, A. P. (2007). *Proc. of IEEE 20th Int. Conf. on Micro Electro Mechanical Systems, MEMS.*, 643-646.

[33] Ivashchenko, V. I., Dub, S. N., Porada, O. K., Ivashchenko, L. A., Skrynskyy, P. L., & Stegniy, A. I. (2006). *Surf. Coat. Technol.*, 200(22-23), 6533-6537.

[34] Behnel, N., Fuchs, T., & Seidel, H. (2009). *Proc. of Int. Conf. on Solid-State Sens., Act. and Microsyst., TRANSDUCERS*, 2009, 740-742.

[35] Chung, C. K., Tsai, M. Q., Tsai, P. H., & Lee, C. (2005). *J. Micromech. Microeng.*, 15(1), 136-142.

[36] Iliescu, C., Tay, F. E. H., & Wei, J. S. (2006). *J. Micromech. Microeng.*, 16(4), 869-874.

[37] Iliescu, C., Chen, B., Poenar, D. P., & Lee, Y. Y. (2008). *Sens. Actuator B-Chem.*, 129(1), 404-411.

[38] Tanaka, S., Rajanna, K., Abe, T., & Esashi, M. (2001). *J. Vac. Sci. Technol. B*, 19(6), 2173-2176.

[39] Chabert, P. (2001). *J. Vac. Sci. Technol. B*, 19(4), 1339-1345.

[40] Schmid, U., Eickhoff, M., Richter, C., Krotz, G., & Schmitt-Landsiedel, D. (2001). *Sens. Actuator A-Phys.*, 94(1-2), 87-94.

[41] Gao, M. B. J., Wijesundara, C., Carraro, R. T., Howe, , & Maboudian, R. (2004). *IEEE Sens. J.*, 4(4), 441-448.

[42] Senesky, D. G., & Pisano, A. P. (2010). *Proc. of 23rd IEEE Int. Conf. on Micro Electro Mechanical Systems (MEMS)*, 352-355.

[43] Pandraud, H. T. M., Pham, P. J., French, P. M., & Sarro, . (2007). *Optics & Laser Technology*, 39(3), 532-536.

[44] Williams, K. R., Gupta, K., & Wasilik, M. (2003). *J. Microelectromech. Syst.*, 12(6), 761-778.

[45] Iliescu, C., Taylor, H., Avram, M., Miao, J., & Franssila, S. (2012). *Biomicrofluidics*, 6(1), 016505-016516.

[46] Iliescu, C., Chen, B., & Miao, J. (2008). *Sens. Actuator A- Phys.*, 143(1), 154-161.

[47] Iliescu, C., Jing, J., Tay, F. E. H., Miao, J., & Sun, T. (2005). *Surf. Coat. Tech.*, 198(1-3), 314-318.

[48] Berthold, F., Laugere, H., Schellevis, C. R., De Boer, M., Laros, R. M., Guijt, P. M., & Sarro, M. J. (2002). *Vellekoop Electrophoresis*, 23(20), 3511-3519.

[49] Iliescu, F. E. H., Tay, J. M., & Miao, . (2007). *Sens. Actuator A-Phys.*, 133(2), 395-400.

[50] Zhang, X., Guo, H., Chen, Z., Zhang, G. B., & Li, Z. H. (2007). *J. Micromech. Microeng.*, 17(4), 775-780.

[51] Poenar, P., Iliescu, C., Carp, M., Pang, A. J., & Leck, K. J. (2007). *Sens. Actuator A-Phys.*, 139(1-2), 162-171.

[52] Zorman, A., & Barnes, A. C. (2012). *in Silicon Carbide Biotechnology*, Elsevier, Oxford, 351-376.

[53] Sharpe, W. N., Jr., Jadaan, O., Beheim, G. M., Quinn, G. D., & Nemeth, N. N. (2005). J. Microelectromech. Syst. ., 14(5), 903-913.

[54] Ashurst, W. R., Wijesundara, M. B. J., Carraro, C., & Maboudian, R. (2004). *Tribology Letters*, 17(2), 195-198.

[55] Flannery, F., Mourlas, N. J., Storment, C. W., Tsai, S., Tan, S. H., Heck, J., Monk, D., Kim, T., Gogoi, B., & Kovacs, G. T. A. (1998). *Sens. Actuator A-Phys.*, 70(1-2), 48-55.

[56] Summers, J. B., Scardelletti, M., Parro, R., & Zorman, C. A. (2007). *in MEMS/MOEMS Components and Their Applications IV, edited by S. A. Tadigadapa, R. Ghodssi and A. K. Henning, Proc. Spie-Int Soc Optical Engineering*, 6464, H4640.

[57] Taylor, D., Boning, C., & Iliescu, . (2011). *J. Micromech. Microeng.*, 21(6).

[58] Gao, X., Yeo, L. P., Chan-Park, M. B., Miao, J. M., Yan, Y. H., Sun, J. B., Lam, Y. C., & Yue, C. Y. (2006). *J. Microelectromech. Syst.*, 15(1), 84-93.

[59] Pakula, L. S., Yang, H., Pham, H. T. M., French, P. J., & Sarro, P. M. (2004). *J. Micromech. Microeng.*, 14(11), 1478-1483.

[60] Carreño, M. N. P., & Lopes, A. T. (2004). *J. Non-Crystalline Solids*, 338-340(0), 490-495.

[61] Carreno, M. N. P., Alayo, M. I., Pereyra, I., & Lopes, A. T. (2002). *Sens. Actuator A-Phys.* [2-3], *100* [2-3], 295-300.

[62] Ni, M., Tong, W. H., Choudhury, D., Rahim, N. A. A., Iliescu, C., & Yu, H. (2009). *Int. J. Mol. Sci.*, 10(12), 5411-5441.

[63] Zhang, S., Tong, W., Zheng, B., Susanto, T. A. K., Xia, L., Zhang, C., Ananthanarayanan, A., Tuo, X., Sakban, R. B., Jia, R., Iliescu, C., , K., Chai, H., Mc Millian, M., Shen, S., Leo, H., & Yu, H. (2011). *Biomaterials*, 32(4), 1229-1241.

[64] Ciarlo, D. R. (2002). *Biomed. Microdev.*, 4(1), 63-68.

[65] Wei, S., Kwong, J., Gaughwin, P., Avram, M., & Iliescu, C. (2009). *Int. J. Comp. Mat. Science Surface Eng.*, 2(3-4), 268-281.

[66] Iliescu, C., Wei, J., Chen, B., & Ong, P. L. (2008). *Rom. J. Inform. Sci. Technol.*, 11(2), 167-176.